17th IEEE International Conference on Advanced Thermal Processing of Semiconductors – RTP 2009

Non-contact, Non-destructive Characterization of Ge Content and SiGe Layer Thickness using Multi-wavelength Raman Spectroscopy

Woo Sik Yoo, Takeshi Ueda, Toshikazu Ishigaki and Kitaek Kang
WaferMasters, Inc.
246 East Gish Road
San Jose, CA 95112 USA

Abstract **–** Design and performance of a newly developed multi-wavelength, micro Raman spectroscopy system for non-contact and non-destructive characterization of semiconductor materials are introduced. The thickness and Ge content of $Si_{1-x}Ge_x$/Si were estimated from the multi-wavelength Raman measurement results and compared to those values obtained from X-ray diffraction (XRD) and X-ray reflectance (XRR) measurements for cross-reference. Both the thickness and Ge content of $Si_{1-x}Ge_x$/Si measured by Raman spectroscopy and X-ray techniques are in excellent agreement. In addition to the non-contact and non-destructive nature of Raman spectroscopy, the multi-wavelength excitation capability of the system, with high spectral and spatial resolution, are very attractive and powerful for characterization of advanced semiconductor materials, such as $Si_{1-x}Ge_x$/Si and strained Si, and process optimization.

I. INTRODUCTION

The enhanced electron and hole mobility of strained Si and strained $Si_{1-x}Ge_x$/Si makes them very attractive as candidate materials for high performance semiconductor devices, such as high speed CMOS and HBT devices [1-6]. The thickness of a $Si_{1-x}Ge_x$ layer, its Ge content and crystallinity of the $Si_{1-x}Ge_x$/Si determine the amount of strain and the enhancement of the carrier transport properties. Electrical properties of device performance in strained Si and strained $Si_{1-x}Ge_x$/Si can only be measured after the completion of device fabrication. For process optimization and quality control, it is important to establish in-line, non-destructive $Si_{1-x}Ge_x$/Si characterization and monitoring techniques.

Raman spectroscopy has been used in characterizing various semiconductor materials in terms of carrier concentration, impurity content, composition, crystal structure, crystal orientation, temperature and mechanical strain since the early 1970's [7-9]. Despite the attractive capabilities of Raman spectroscopy, its practical applications were limited to academic research and failure analysis using small samples. In addition to the lack of availability of automatic handling of large size wafers, measurement accuracy, repeatability, spectral resolution, spatial resolution and calibration related issues have been preventing practical application of this technique from achieving wide acceptance as an in-line monitoring technique in the industry. Since the introduction of strain and Ge in Si for device performance enhancement, Raman spectroscopy has been revisited by many researchers as a preferred, non-destructive stress/strain characterization technique for semiconductor materials for the last few years [3-20].

We have designed a special polychromator-based multi-wavelength micro-Raman spectroscopy system (MRS-300) to overcome the common issues with conventional Raman measurement systems. Preliminary results on the performance of the newly designed Raman system (MRS-300) and Raman characterization of mechanically stressed Si and $Si_{1-x}Ge_x$/Si were reported previously [18].

In this paper, we have demonstrated non-contact and non-destructive characterization of the thickness and Ge content in $Si_{1-x}Ge_x$/Si using the MRS-300 system in a highly accurate and repeatable manner. The application of the MRS-300 as an in-line process monitoring tool was also examined by collecting data on long term measurement stability and repeatability. An example of an in-line application of the MRS-300 system is also given.

II. EXPERIMENT

A. Multi-wavelength Raman Spectroscopy (MRS-300)

Semiconductor materials including Si, $Si_{1-x}Ge_x$/Si and Ge have their own spectral responses based on bandgap, impurity and surface conditions. Light with photon energy greater than the bandgap of a semiconductor is partially absorbed when illuminated on the semiconductor. The shorter wavelength photons are generally absorbed efficiently by semiconductors. The rate of intensity attenuation in the depth direction is higher for the shorter wavelengths, with higher photon energy. The absorption coefficient is higher for light with these short wavelengths and higher photon energy. As a consequence, the light penetration depth, as well as the probing depth of Raman characterization can be adjusted by selecting appropriate excitation wavelengths for depth profiling.

We have designed the MRS-300 system as an in-line stress/strain monitoring system. The system has three thermoelectrically cooled, charge coupled device (CCD)

978-1-4244-3815-0/09/$25.00 ©IEEE

cameras that can measure Raman peaks from three different excitation wavelengths without any disruption (i.e., without scanning the monochromator or switching the excitation laser) (Fig. 1). The measurement capability of the system is summarized in Fig. 2. Three major spectral lines (457.9, 488.0 and 514.5nm) from a multi-wavelength Ar^+ ion laser are used as the excitation source. By selecting the wavelength of the excitation laser, the crystal quality, stress and strain in the depth direction can be characterized [10-13, 18].

Microscopic Raman scattering is a powerful, non-destructive technique for characterizing crystallinity and the degree of stress/strain of the crystal [3-13]. For this purpose intensity, shift, and full-width-at-half-maximum (FWHM) of Raman signals are measured.

B. Reference Si (100) and $Si_{1-x}Ge_x$/Si (100) Samples

As a measurement reference, a stress-free Si (100) wafer was prepared. A large number (>200) of epitaxially grown $Si_{1-x}Ge_x$/Si (100) samples with different Ge content and different $Si_{1-x}Ge_x$ layer thickness were prepared and characterized. The Ge content was varied from 15 to 32 atomic percent. The thickness of the $Si_{1-x}Ge_x$ layer was in the range of 40 nm ~ 120 nm. A few samples had a thin NiPt layer on top of the $Si_{1-x}Ge_x$/Si (100) for silicidation.

III. RAMAN RESULTS AND DISCUSSIONS

A. Measurement Resolution, Accuracy and Repeatability

In any scientific experiment or monitoring for quality control applications, establishing measurement accuracy and repeatability is essential. The system requirements of measurement resolution, accuracy and repeatability often conflict with the desire for flexibility, productivity, compactness as well as other economic factors. System designers are often forced to make compromised decisions due to cost factors and market competitiveness of developing equipment, rather than addressing scientific or engineering limitations.

In the design phase of the MRS-300 system, we have mainly focused on achieving the highest possible measurement resolution, accuracy, repeatability, excitation wavelength flexibility and productivity. After careful analysis and review of possible design options and technical merits/demerits of individual design options, the polychromator-based, multi-wavelength, micro-Raman spectroscopy system design was chosen. The unique features of a very long focal length (2.0m) focusing mirror with wide spectrum coverage, three CCD cameras for measuring Raman signals from three individual excitation wavelengths, and the elimination of moving parts in the spectrograph, made the realization of high spectral resolution, accuracy, repeatability, excitation wavelength flexibility and productivity possible.

In conventional monochromator-based Raman systems, frequent system calibration is required (daily and between excitation wavelength switching). However, the unique no-moving part design of the MRS-300 system was able to minimize the common mechanical problems in traditional Raman systems, namely: the uncertainties in absolute wavenumber of Raman signals due to calibration errors, optical misalignment due to vibration and backlash of moving parts (mainly diffraction grating(s)). The MRS-300 system design also enabled multi-wavelength Raman measurements from the same measurement site without refocusing or calibrating between switching of excitation wavelengths for different penetration depths. This innovative design aspect of the MRS-300 has upgraded the reliability of Raman measurement and enables the in-line monitoring of properties of Si (stress, strain, Ge content, $Si_{1-x}Ge_x$ layer thickness etc.) for process development, process optimization and quality control.

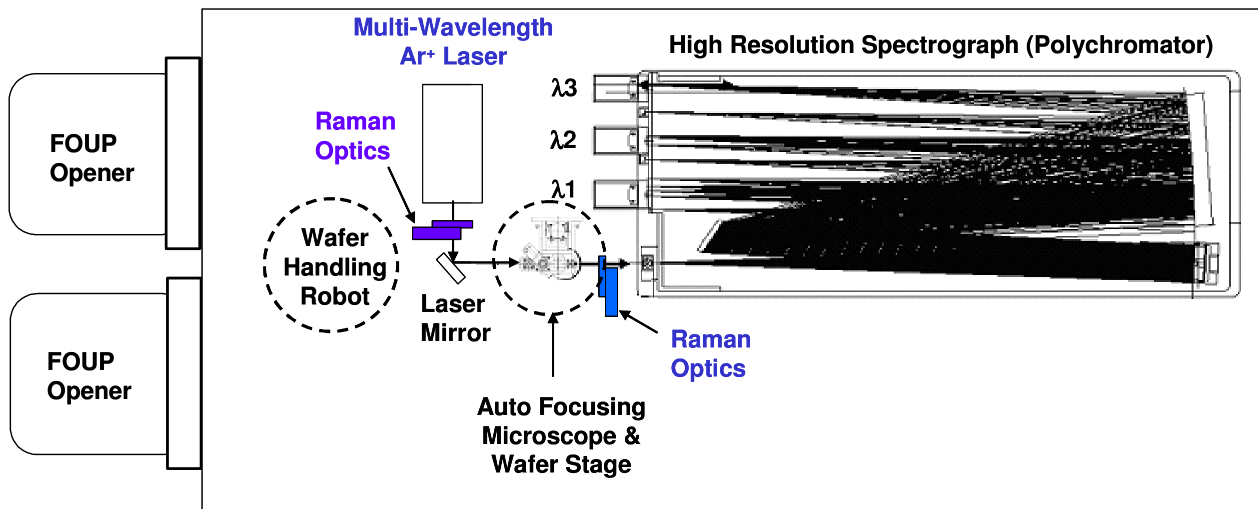

Fig. 1. Schematic illustration of multi-wavelength Raman spectroscopy (MRS-300) system.

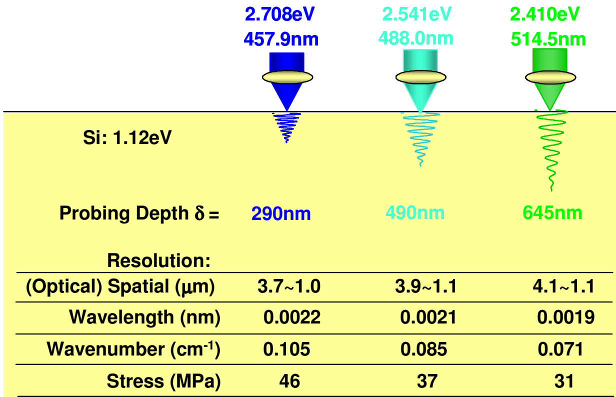

Fig. 2. Summary of measurement capability of the MRS-300 with various excitation wavelengths of the multi-wavelength Ar^+ laser.

Raw data from Raman signals from bare Si (100) measured using the MRS-300 system under various wavelength excitations is shown in Fig. 3. Raman signals from all three excitation wavelengths are centered at ~520.3cm^{-1} and are highly symmetrical. The symmetry of the Raman signal suggests that the MRS-300 system has extremely low distortion error and confirms that the quality of the reference Si (100) measurement is excellent. Since the pixel size of all CCD cameras are the same (13.5μm x 13.5μm), data points are much denser in longer wavelength Raman data after converting the same pixel bandwidth into wavenumber, Raman shift or Raman frequency. The wavenumber resolution exceeds 0.105cm^{-1} in all three wavelengths (457.9nm, 488.0nm and 514.5nm) before curve fitting. Since the 0.1cm^{-1} shift of the Raman signal from Si corresponds to ~40MPa, the high wavenumber or spectral resolution and high measurement repeatability of at least ~0.1cm^{-1}, before curve fitting, is conducive for accurate stress and strain analysis of combinations of Si and $Si_{1-x}Ge_x$ materials used in advanced high performance devices.

For verification of measurement repeatability with the MRS-300 system, Raman signals from the same reference Si (100) sample were measured under the three wavelength excitations every day for a period of one month (Fig. 4). Variations in Raman shift and FWHM at all three excitation wavelengths during the monitoring period of one month was less than 0.05cm^{-1}. Hence, the designed performance specifications of the MRS-300 system design were experimentally verified. With the high spectral resolution, measurement accuracy and repeatability of MRS-300 system, reliable Raman studies on stress, strain and the effect of Ge became possible. Because of its accuracy and repeatability, in-line Raman signal monitoring is very useful for determining process variations within wafer, wafer-to-wafer and system-to-system. It can provide additional insights into hidden material, process and equipment problems.

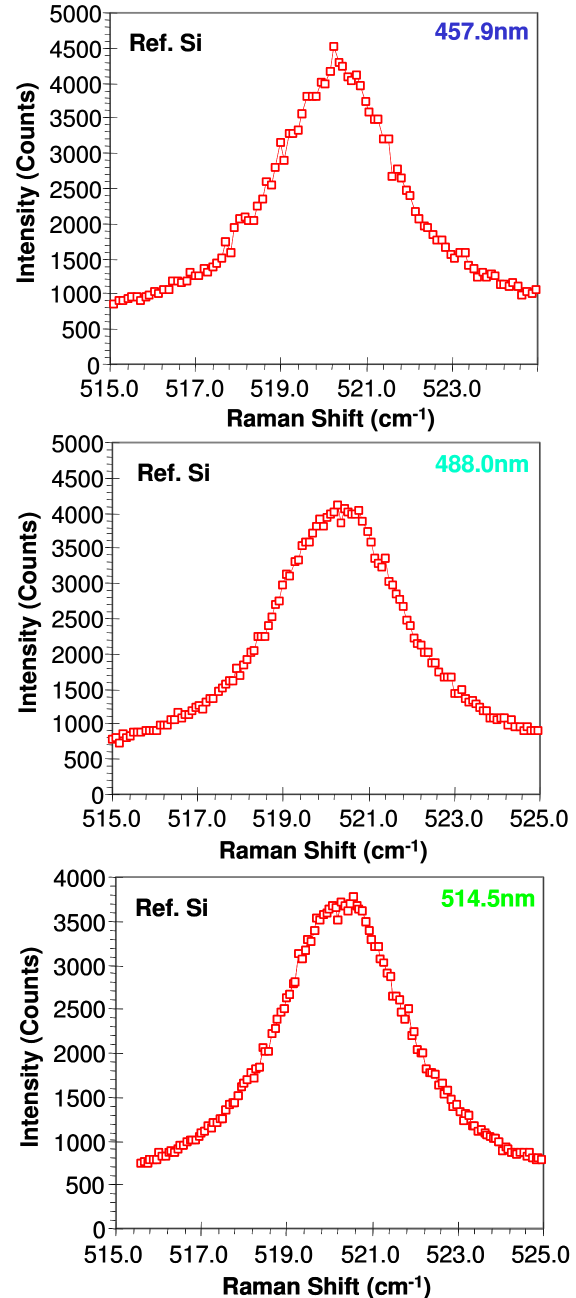

Fig. 3. Raw Raman measurement data taken using the MRS-300 system under 457.9nm, 488.0nm and 514.5nm excitation, demonstrating very high wavenumber resolution.

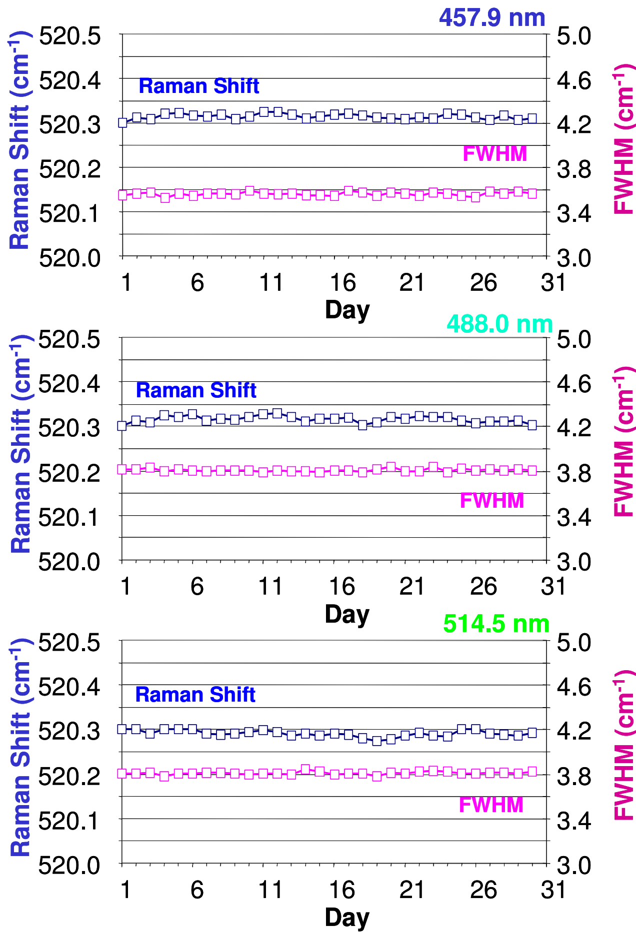

Fig. 4. Measurement repeatability data collected from MRS-300 system for a period of one month.

B. $Si_{1-x}Ge_x$/Si (100) Samples

Carrier mobility enhancement in strained Si, as well as in strained $Si_{1-x}Ge_x$, is strongly dependant on the magnitude of strain in the channel region and can be modulated by controlling the Ge content below, or in the channel region. Accurate measurement of strain and/or Ge content is extremely important for process optimization and manufacturing devices with high performance uniformity, repeatability and reliability. Raman spectroscopy has been proposed by many research groups as a promising characterization technique [1, 3-18].

A sample of stress-free blanket Si (100), and a large number of $Si_{1-x}Ge_x$/Si (100) samples with different Ge content, ranging from 15 to 32 atomic percent and different $Si_{1-x}Ge_x$ layer thicknesses ranging from 40nm to 120nm were prepared. Raman signals were measured under 457.9nm, 488.0nm and 514.5nm excitation. As seen in Fig. 6, all four $Si_{1-x}Ge_x$/Si (100) samples with different Ge content showed a second peak, on the left (the lower wavenumber side) of the Raman peak from bulk Si, regardless of excitation wavelength. The second peak is identified as a Raman signal from Si-Si bonds in $Si_{1-x}Ge_x$. As the Ge content increases, the second peak, from the Si-Si bonds in $Si_{1-x}Ge_x$, shifts towards the lower wavenumber side. This phenomenon is well known and the separation of the second peak of $Si_{1-x}Ge_x$ from the bulk Si peak is often used to determine the amount of strain and/or Ge content in $Si_{1-x}Ge_x$ [3-6, 18].

C. Ge Content of $Si_{1-x}Ge_x$/Si (100)

As seen in Fig. 7, a monotonic increase of the separation of the second peak of $Si_{1-x}Ge_x$ from the bulk Si peak occurs at a rate of $-0.35cm^{-1}$/Ge atm% at all three excitation wavelengths [18]. Ge content measurement values were in good agreement with the Ge content measured by x-ray diffraction (XRD) within measurement error (<0.1atm%). By measuring the separation between two peaks, non-contact and non-destructive characterization of stress and/or Ge content of $Si_{1-x}Ge_x$/Si can easily be accomplished in-line. Raman measurements of samples between process steps can be used as a process quality assurance metric or for important inputs for process development, optimization and qualification. Both within-wafer and wafer-to-wafer variations in Raman peak positions (shifts), FWHMs and separation between the two peaks provide immediate feedback of strain and/or Ge content variation in the sample. Raman measurement results under different excitation wavelength also provide the same valuable information at different depths into the wafer.

D. $Si_{1-x}Ge_x$ Layer Thickness of $Si_{1-x}Ge_x$/Si (100)

The bandgap of $Si_{1-x}Ge_x$ decreases as Ge content increases. The light absorption coefficient at a given wavelength in visible wavelength region increases as the bandgap narrows (i.e. Ge content increases). The probing depth of $Si_{1-x}Ge_x$ is shallower than that of bulk Si at a given excitation wavelength (457.9nm, 488.0nm and 514.5nm). Since the narrow bandgap $Si_{1-x}Ge_x$ layer on Si substrate works as an attenuation filter for the excitation wavelength, the Raman peak intensity ratio of I_{Si-Si}/I_{Si} is strongly affected by the $Si_{1-x}Ge_x$ layer thickness and its Ge content.

The Raman peak intensity ratio of I_{Si-Si}/I_{Si} in $Si_{0720}Ge_{0.28}$ /Si (100) under various excitation wavelengths is plotted (Fig.8) as a function of $Si_{0.72}Ge_{0.28}$ layer thickness. The thickness of $Si_{0.72}Ge_{0.28}$ layers was verified by x-ray reflectance (XRR) measurement data. Since the light absorption coefficient of $Si_{1-x}Ge_x$ is higher in the short wavelength region at a given Ge content, the shortest excitation wavelength provides the highest

Raman peak intensity ratio (I_{Si-Si}/I_{Si}) change with change in $Si_{1-x}Ge_x$ layer thickness. Unlike conventional characterization techniques such as XRD, XRR etc., multi-wavelength micro-Raman spectroscopy can determine Ge content, stress/strain, crystallinity and $Si_{1-x}Ge_x$ layer thickness with sub-micron spatial resolution in a single measurement.

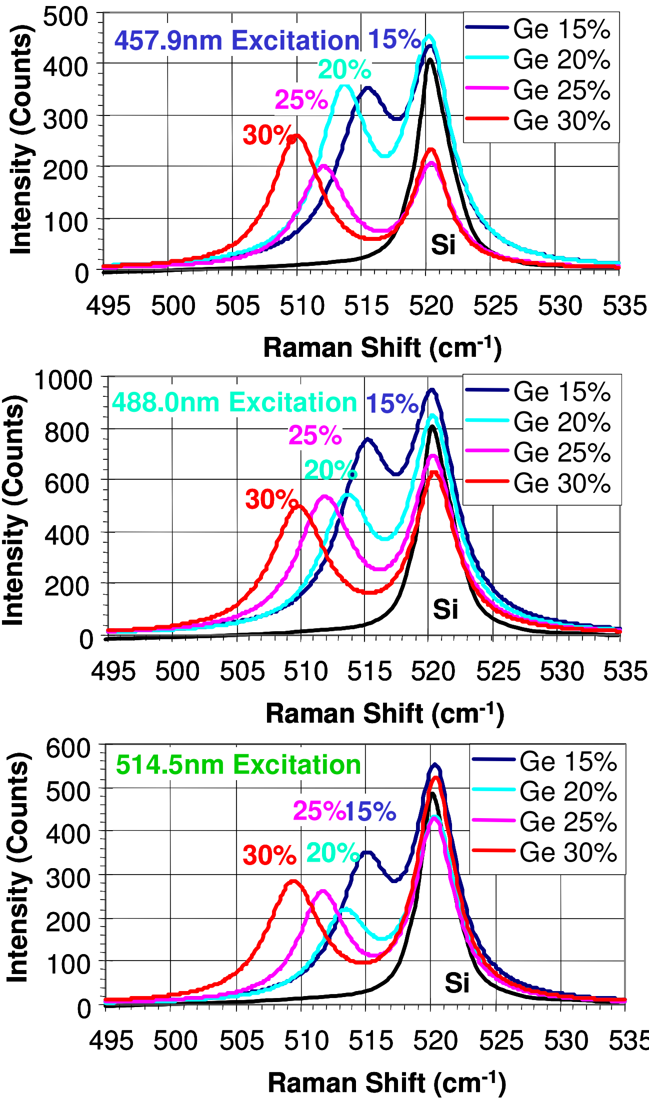

Fig. 6. Si and Si-Si Raman peaks from $Si_{1-x}Ge_x$ (x = 0, 0.15, 0.20, 0.25 and 0.30) samples under 457.9nm, 488.0nm and 514.5nm excitations.

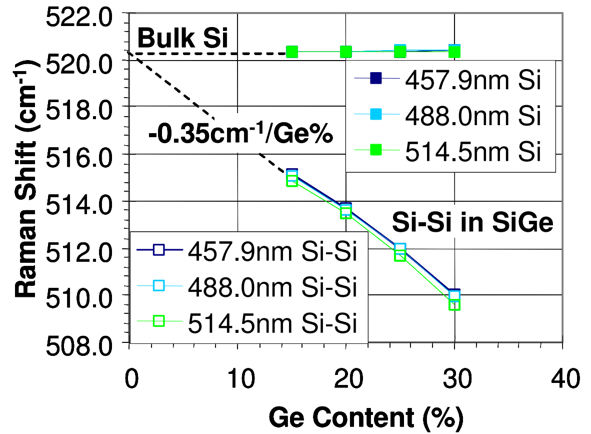

Fig. 7. Frequency shift of Si and Si-Si Raman peaks as a function of Ge content measured from $Si_{1-x}Ge_x$ (x = 0, 0.15, 0.20, 0.25 and 0.30) samples under 457.9nm, 488.0nm and 514.5nm excitations.

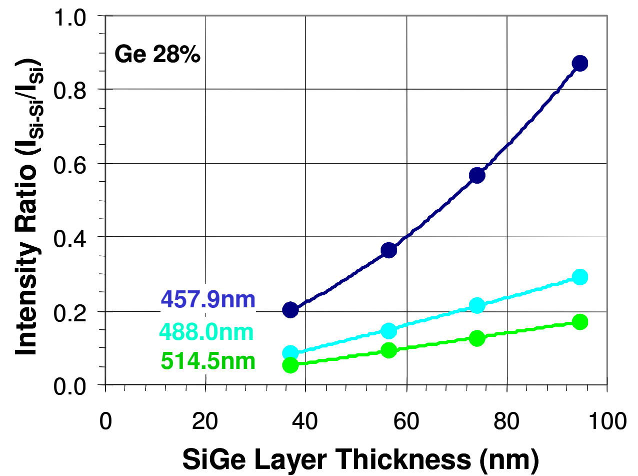

Fig. 8. Raman signal intensity ratio of I_{Si-Si}/I_{Si} measured from $Si_{0.72}Ge_{0.28}$/Si (100) samples with various $Si_{0.72}Ge_{0.28}$ layer thicknesses under different excitation wavelengths.

E. Comprehensive Characterization of $Si_{1-x}Ge_x$/Si (100)

Contour maps of Raman measurement results from a $Si_{0.80}Ge_{0.20}$/Si (100) sample were plotted in terms of Raman peak positions from Si-Si in $Si_{0.80}Ge_{0.20}$ and Si, FWHMs of Raman peaks and estimated Ge content. Within sample variations (non-uniformity) of various material characterization aspects (measurement factors) can be visualized by multi-wavelength micro-Raman mapping. As seen in Fig. 9, variations in Ge content and crystallinity (FWHM) of the Si substrate due to the effect of $Si_{0.80}Ge_{0.20}$ top layer are obvious. Only the 488.0nm Raman measurement result is shown due to space

limitation. The variations of material properties in the depth direction was also observed by comparing contour maps generated using analyzed Raman data from different excitation wavelengths.

IV. SUMMARY

The design concept of a polychromator-based multi-wavelength Raman spectroscopy system (MRS-300) is described. The system is specially designed for non-destructive, material and process characterization applications in the semiconductor industry. The unique design features of the MRS-300 system are reviewed and compared with the common issues with conventional Raman measurement systems. The performance of the MRS-300 system and non-destructive nature of the tests of lattice stress/strain and Ge content were demonstrated using mechanically stressed Si samples and epitaxially grown $Si_{1-x}Ge_x$ samples. The capability for very high measurement resolution ($0.105cm^{-1}$/pixel or better), accuracy repeatability ($0.05cm^{-1}$ or better) and overall repeatability ($0.05cm^{-1}$ or better) of the system were demonstrated at all three excitation wavelengths (457.9nm, 488.0nm and 514.5nm). This work makes extensive use of the unique ability of the MRS-300 to make measurements at different depths at exactly the same location. The use of MRS-300 applications for in-line process monitoring was introduced with an example of long term measurement stability and repeatability data.

The thickness and Ge content of $Si_{1-x}Ge_x/Si$ were derived from the multi-wavelength Raman measurement results and compared to those values obtained from X-ray diffraction (XRD) and X-ray reflectance (XRR) measurements for cross-reference. Both the thickness and Ge content of $Si_{1-x}Ge_x/Si$ measured by Raman spectroscopy and X-ray techniques are in excellent agreement. In addition to the non-contact and non-destructive nature of Raman spectroscopy, the multi-wavelength excitation capability of the system with high spectral and spatial resolution is very attractive and powerful for characterization of advanced semiconductor materials, such as $Si_{1-x}Ge_x/Si$ and strained Si, and process optimization.

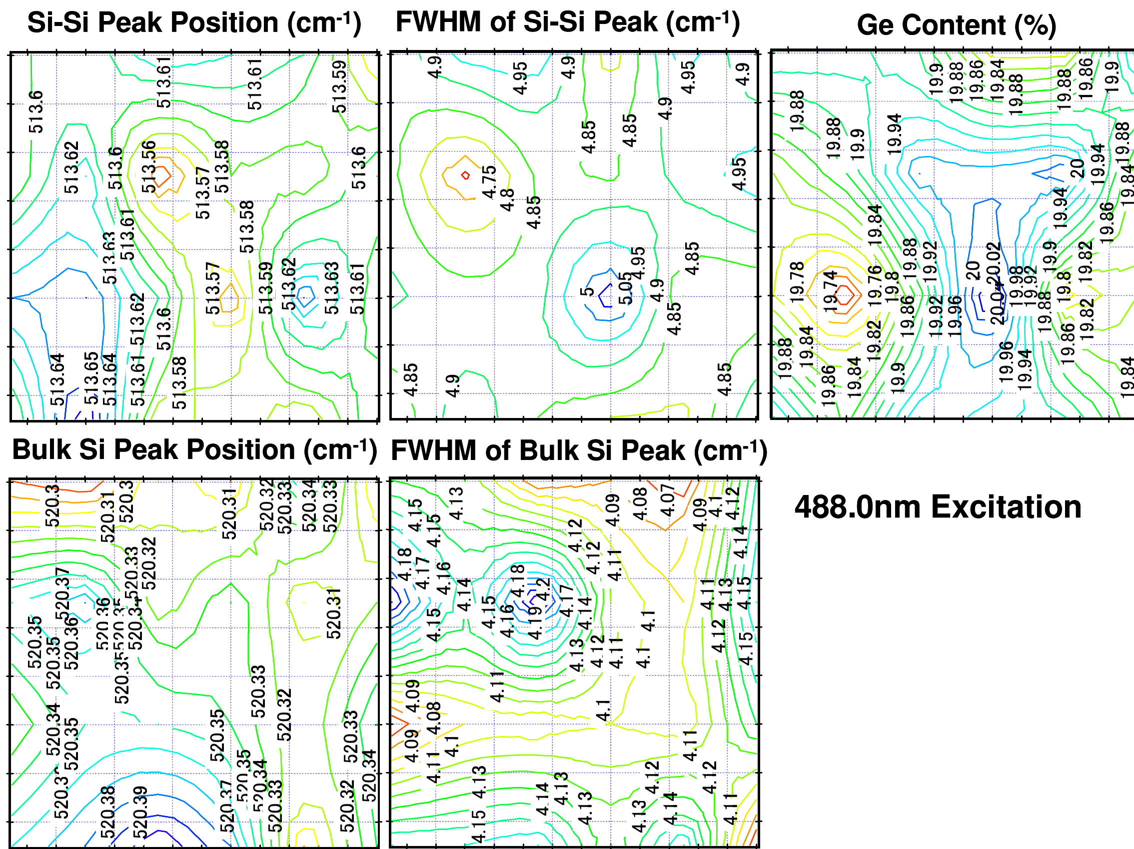

Fig. 9. Contour maps of Raman measurement results: Raman peak positions from Si-Si in $Si_{0.80}Ge_{0.20}$ and Si, FWHMs of Raman peaks and estimated Ge content. (Only 488.0nm excited Raman measurement results are shown due to space limitations.)

REFERENCES

[1] F. Meyer, M. Zafrany, M. Eizenberg, R. Beserman, C. Schwebel and C. Pellet, J. Appl. Phys., **70 (8)** (1991) 4268.

[2] M. Khater, T. Adam, J.S. Rieh, K. Schonenberg, F. Pagette, K. Stein, S.J. Jeng, D. Ahlgren and G. Freeman, ECS Transactions, **3 (7)** (2006) 341.

[3] L.H. Wong, C.C. Wong, J. P. Liu, D. K. Shon, L. Chan, L.C. Hsia, H. Zang, Z. H. Ni and Z.X. Shen, Jpn. J. Appl. Phys., **44** (2005) 7922.

[4] M. Belyansky, A. Domenicucci, N. Klymko, J. Li and A. Madan, Solid State Technology, **52 (2)** (2009) 26.

[5] J.P. Liu, K. Li, S.M. Pandey, F.L. Benistant, A. See, M.S. Zhou, L.C. Hsia, R. Schampers and D. O. Klenov, Appl. Phys. Lett., **93** (2008) 221912.

[6] J. Kasim, Y. Ting, Y.Y. Meng, L.J. Ping, A. See, L.L. Jong, and S.Z. Xiang, Optics Express, **16** (2008) 7976.

[7] I. De Wolf, Spectroscopy Europe, **15/2** (2003) 6.

[8] H. Harima, Proc. 14th IEEE Int. Conf. on Advanced Thermal Processing of Semiconductors, **RTP 2006**, 117.

[9] H. Harima, S. Nakashima, J.M. Carulli, C.P. Beetz, Jr., and W.S. Yoo, Jpn. J. Appl. Phys., **36** (1997) 5525.

[10] S. Nishibe, T. Sasaki, H. Harima, K. Kisoda, T. Yamazaki and W.S. Yoo, Proc. 14th IEEE Int. Conf. on Advanced Thermal Processing of Semiconductors, **RTP 2006**, 211.

[11] M. Yoshimoto, H. Nishigaki, H. Harima, T. Isshiki, K. Kang and W.S. Yoo, J. Electrochem. Soc., **153** (2006) G697.

[12] W. S. Yoo, T. Ueda, J. Kajiwara, T. Ishigaki and K. Kang, ECS Transactions, **13 (1)** (2008) 359.

[13] W.S. Yoo, T. Ueda and K. Kang, Ext. Absts. Int. Conf. on Solid State Devices and Materials (2008) 376.

[14] A. Ogura, K. Yamasaki, D. Kosemura, S. Tanaka, I. Chiba and R. Shimidzu, Jpn. J. Appl. Phys., **45** (2006) 3007.

[15] M. Yoshikawa, M. Murakami, K. Matsuda, R. Sugie, H. Ishida and R. Shimizu, Jpn. J. Appl. Phys., **45** (2006) L486.

[16] K. Kodera, T. Iguchi, N. Tsuchiya, M. Tamura, S. Kakinuma, N. Naka and S. Kashiwagi, Jpn. J. Appl. Phys., **47** (2008) 2506.

[17] K. Sawano, N. Usami, K. Arimoto, K. Nakagawa and Y. Shiraki, Jpn. J. Appl. Phys., **44** (2005) 8445.

[18] W.S. Yoo, T. Ueda and K. Kang, Ext. Abs. the 9th International Workshop on Junction Technology 2009, **IWJT 2009**, 79.

[19] T.A. Langdo, M.T. Currie, A. Lochtefeld, R. Hammond, J.A. Carlin, M. Erdtmann, G. Braithwaite, V.K. Yang, C.J. Vineis, H. Badawi and M.T. Bulsara, Appl. Phys. Lett., **82** (2003) 4256.

[20] T.S. Drake, C. Ní Chléirigh, M.L. Lee, A.J. Pitera, E.A. Fitzgerald, D.A. Antoniadis, D.H. Anjum, J. Li, R. Hull, J.L. Hoyt, Appl. Phys. Lett., **83** (2003) 875.